# Origin of the variable-range vortex hopping in $Bi_2Sr_2Ca_{1-x}Y_xCu_2O_8$ with columnar defects

J. C. Soret,* V. Ta Phuoc, L. Ammor, A. Ruyter, R. De Sousa, and E. Olive
*Laboratoire d'Electrodynamique des Matériaux Avancés,† Université F. Rabelais, UFR Sciences, Parc de Grandmont, 37200 Tours, France*

G. Villard, A. Wahl, and Ch. Simon
*Laboratoire CRISMAT,‡ ISMRA, 6 Boulevard du Maréchal Juin, 14050 Caen Cedex, France*
(Received 28 April 1999)

We report on the vortex transport in $Bi_2Sr_2Ca_{1-x}Y_xCu_2O_8$ single crystals irradiated in a parallel direction with the $c$ axis with 5.8-GeV Pb ions at fluences of $3.75\times10^{10}\,\mathrm{cm}^{-2}$ and $7.5\times10^{10}\,\mathrm{cm}^{-2}$. A detailed investigation of the vortex transport using current-voltage measurements is carried out with the magnetic field applied along the $c$ axis. First, we investigate the critical behavior of the linear and nonlinear conductivity near the Bose-glass melting line. We obtain field and sample-independent critical exponents $z'$ and $\nu'$ consistent with a compressible Bose glass (i.e., $\nu_\parallel = 2\nu_\perp \equiv 2\nu'$). Using the values $z' = 5.28 \pm 0.05$ and $\nu' = 1.04 \pm 0.06$, the data collapse into two single-scaling functions. Second, we report on conductivity measurements over a wide filling factor ($B/B_\phi$) range from 0.04 up to 0.9 within the Bose-glass phase. Our data provide support for a variable-range hopping mechanism for low current densities, in accordance with the ideas of Nelson and Vinokur [Phys. Rev. B **48**, 13 060 (1993)]. We determine a glass exponent value of 1/3 for all the filling factors investigated at large ratios of the penetration depth to the average defect distance ($\lambda_{ab}/d \sim 10$). This finding implies that no Coulomb gap occurs in the pinning energy spectrum. Furthermore, our results show that for low filling factors ($<1/2$) the on-site disorder plays a major role in the bandwidth of flux-binding energies. Finally, the appearance of a well-defined crossover near half filling is consistent with the field $B^*$ separating the strongly pinned Bose-glass regime from the weakly pinned Bose-glass regime.

## I. INTRODUCTION

The discovery of the high-$T_c$ cuprates has triggered an extensive study of the statics and dynamics of the flux line lattices in type-II superconductors.[1] Static disorder plays a crucial role on the structure of the Abrikosov vortex lattice as predicted a long time ago by Larkin.[2] It is now realized that combined effects between temperature, elasticity, and long-range vortex-vortex repulsion yield to a remarkable variety of states for the flux line lattice when it is driven by the Lorentz force over a random medium.[3–5] The nature of these vortex phases and how they depend on the type and strength of the disorder are far from being completely elucidated. It is generally agreed that quenched disorder produces a glassy low-temperature state separated by a phase transition from a liquid high-temperature state. At zero temperature there is a depinning transition from a pinned state where the average velocity of lines is zero to a sliding state at a critical current density $J_c$. The transition is washed out by the temperature, and thus the average velocity of lines is finite for all driving current densities. For low temperatures and current densities well below the zero-temperature critical current, i.e., $J \ll J_c$, the dynamics of the flux line system is determined by thermally activated jumps of flux bundles over the pinning energy barriers separating different metastable states. In this so-called creep regime, the favorable metastable states are always distant and separated by a diverging barrier $U(J) \sim (J_c/J)^\mu$. The value of the positive glass exponent $\mu$ is determined by the range of $J$,[6] and thus the linear resistivity vanishes even at finite temperatures.[7] Recent theoretical investigations[8–11] on the precise nature of these glassy phases have shown that some weak uncorrelated disorder, such as, for example, atomic impurities,[12] leads to the so-called Bragg glass[8] at low fields undergoing a field-driven transition into a vortex glass[7] or a pinned liquid. This is supported by numerical simulations,[13] by magnetization measurements showing an increase of the effective critical current,[14,15] and by neutron diffraction experiments.[16] In contrast with pointlike impurities, columnar defects, such as those produced by heavy ion irradiations[17] or twin planes, are indeed capable of pinning flux lines over their entire length and thus act as extended disorder, promising stronger pinning effects, as has systematically been observed with all the compounds studied.[18,19] Nelson and Vinokur[20] and Hwa *et al.*[21] have shown that for low temperatures such extended or correlated disorders lead to a variety of glassy vortex phases such as the Bose glass produced by the presence of parallel columnar defects into the superconductor and the splayed glass resulting from a dispersion in the orientation of the columnar defects.

On the basis of the theory of two-dimensional bosons with short-range repulsive interactions moving in a random potentiel at zero temperature,[22] Nelson and Vinokur[20] have studied the influence of random columnar defects on the physics of flux lines parallel to the direction of defects. They have shown that the flux line system exhibits three distinct thermodynamic phases: a vortex liquid at high temperatures undergoing a continuous phase transition at $T_{BG}$ into a Bose-glass characterized by an infinite tilt modulus due to the strong localization of lines on the columnar defects and an incompressible Mott insulator at lower temperatures when the density of flux lines exactly matches the density of co-

 

lumnar defects. In the Bose-glass phase, the dominant vortex transport mechanism for low external currents has been predicted to be the analog of the Mott variable-range hopping.[23] In this scenario, a line hops via the formation of a pair of ''superkinks'' extending from one columnar defect to another unoccupied defect, in general distant with nearly the same energy, such that the thermally assisted tunneling process between the sites is optimized.[20] In the absence of interaction effects, the glass exponent value $\mu = 1/3$ is the very signature for variable-range vortex hopping. Long-range interactions between the lines lead to the distinction of a strongly and a weakly pinned Bose-glass phase separated in the $B$-$T$ plane by the characteristic field $B^*(T)$ introduced in Ref. 20. Moreover, when the density of flux lines is greater than the density of columnar defects, the interactions should also lead to the formation of a state in which the weakly pinned Bose-glass phase coexists with an interstitial vortex ''liquid'' phase.[24] Some of these predictions have been confirmed by experiments on different compounds with columnar defects[25–38] and by numerical simulations.[39,40] Remnants of the Mott insulating phase predicted for short-range interactions at zero temperature have been found.[25,26,40] The irreversibility line of $YBa_2Cu_3O_{7-\delta}$ (YBCO) has been discussed in terms of the Bose-glass melting line,[33] whereas it has rather been related to the crossover line $B^*(T)$ for a highly anisotropic material such as $Bi_2Sr_2CaCu_2O_{8-\delta}$ (BSCCO).[34] Typical creep regimes of the Bose glass have been inferred from magnetization relaxation and transport data;[35–37] on the contrary, it has recently been argued that the vortex creep is dominated by the nucleation of vortex kinks at the sample surface rather than by bulk excitations as half-loops and pairs of ''superkinks.''[41] Many investigations of the critical behavior of physical quantities, such as ac conductivity,[27,28] dc conductivity,[26,29–31,37] and third-harmonic transmissivity,[32] at the onset of the Bose-glass–to–liquid transition, give support to the scaling theory predicted in Ref. 20. Nevertheless, a large dispersion in the reported values for the critical exponents has been found, and furthermore, contrary to theoretical predictions[20] and numerical simulations,[40] some of them imply an incompressible Bose-glass phase just below $T_{BG}$.

In order to clarify further the above issues, a detailed investigation of transport data is carried out in both a BSCCO single crystal and a Y-substituted BSCCO single crystal irradied at different fluences. The experiment is described in the next section. In Sec. III, the universality of the critical behavior of the resistivity around $T_{BG}$ is explored using current-voltage ($I$-$V$) measurements. Both the Bose-glass–to–liquid transition line $T_{BG}(B)$ in the $B$-$T$ plane and the critical exponents $z'$ and $\nu'$ are determined. We show that the scaling forms, obtained in both crystals for different filling factors ($f = B/B_\phi$) ranging over the interval 0.026–0.9, are superimposed on top of each other, and to that end, $z'$ and $\nu'$ happen to be field and sample independent. The exponents $z' = 5.28 \pm 0.05$ and $\nu' = 1.04 \pm 0.06$ are both obtained in this way. We note that such experimental findings are consistent with a true critical behavior along the $T_{BG}(B)$ line. Another important point of this paper is that below $T_{BG}$ a variable-range hopping mechanism is clearly evidenced from the divergence of the conductivity at low currents. A glass exponent value of 1/3, which is typical of a Bose glass with short-range interactions, is obtained for all filling factors $0.026 \leqslant f < 1$. The consequence is that no formation of a Coulomb gap occurs in the strongly underfilled regime at large $\lambda/d \sim 10$. In Sec. IV, the origin of the variable-range hopping mechanism in the underfilled regime ($f < 1/2$) is discussed in terms of bandwidth of the pinning energies arising essentially from on-site disorder. A summary of our results concludes this work.

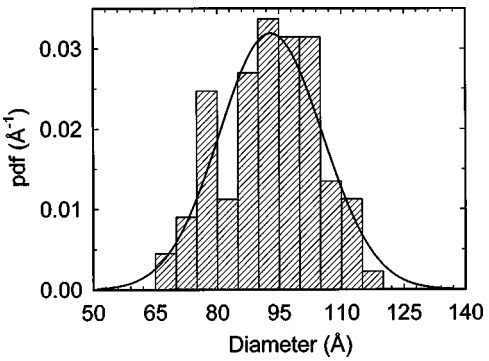


FIG. 1. Data plot of the probability density function (pdf) for the defect diameters. Ordinates are normalized in such a way that the hatched area be equal to unity. The solid line is a Gaussian curve centered at 93 Å with a standard deviation of 12.5 Å.

## II. EXPERIMENTAL METHOD

The experiment has been performed on two irradiated $Bi_2Sr_2Ca_{1-x}Y_xCu_2O_8$ single crystals with $x = 0$ (sample $A$) and $x = 0.36$ (sample $B$) which have been grown by the distinct self-flux methods described in Refs. 42 and 43, respectively. The crystal sizes are approximately equal to $1 \times 1 \times 0.030\,\mathrm{mm}^3$ (sample $A$) and $1.3 \times 1 \times 0.015\,\mathrm{mm}^3$ (sample $B$), with the crystallographic $c$ direction along the shortest dimension. Sample $A$ has a zero-field transition temperature $T_c$ (determined using the inflexion point of the resistive transition) of 89.0 K, while sample $B$ has a $T_c$ value of 91.2 K. For both samples, the resistance as a function of the temperature, $R(T)$, does not exhibit any ''shoulder'' or other anomalies near $T_c$. An estimate of their transition width $\Delta T$, obtained from the width at half-maximum of the $dR/dT$ peak, gives $\Delta T \approx 1.0$–$1.5\,\mathrm{K}$.

Irradiations have been carried out at room temperature with 5.8-GeV Pb ions delivered at the Grand Accélérateur National d'Ions Lourds (GANIL) at Caen. Both crystals have been irradiated along their $c$ axis. The electronic stopping power (~32 keV/nm) of the Pb ions varied by less than 10% within the thickness of the samples and was sufficiently large for producing homogeneous columnar defects throughout the thickness of our crystals.[44] The morphology of the defects has been characterized by high-resolution electron microscopy.[44] The apparent images of tracks, viewed along the [001] direction, reveal circular zones of different diameters. The probability density function of diameters obtained from a sample of 89 tracks is shown in Fig. 1. It can be seen that the diameters have approximately a normal distribution. On the other hand, the global track density, measured from some images recorded for different areas of the crystal, is similar to the incident ion fluence, which is known within a precision of about 10%. The fluences expressed in terms of the matching field $B_\phi$ ($B_\phi = \phi_0/d^2$ where $\phi_0$ is the elemen-

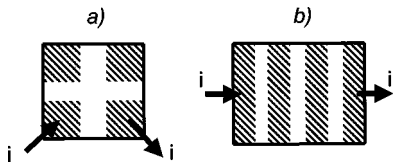


FIG. 2. Sketch of contact geometries. The hatched areas represent the contacts. (a) Sample A: contacts are positioned to its corners and have typical dimensions of $450\times450\ \mu m^2$ with $\sim100$ $\mu$m separation. (b) Sample B: four contacts are put along its length and have typical dimensions of $1000\times275\ \mu m^2$ with $\sim75$ $\mu$m separation.

tary flux quantum and $d$ is the mean distance between defects) are 1.5 T for sample $A$ and 0.75 T for sample $B$.

Electrical contacts have been made by evaporing four Au pads on a face of each crystal and attaching gold wires to those pads with silver epoxy. The whole has then been annealed under air at 400 °C during 30 min without affecting seriously the efficiency of the vortex pinning due to columnar defects.[45] The ensuing contact resistance (per contact including lead resistance) is less than $5\Omega$. The contacts on crystal $B$ are along the length of the sample, whereas for crystal $A$ they are positioned to its corners due to sample size limitations, as schematically shown in Fig. 2. It was recently suggested[46] that such contact arrangements, in which the vortices follow trajectories crossing the edges, are unsuitable for probing bulk pinning in *clean* BSCCO crystals due to strong surface barriers, which are found to dominate the transport properties. Nevertheless, it is generally agreed that the presence of columnar defects in this material produces bulk pinning more effectively than the surface effects.[33–37] We therefore consider that both contact geometries used in our experiment do not influence the results reported below. The resistances at $T=100\,\mathrm{K}$ are $R(100\,\mathrm{K})\approx0.11\,\Omega$ and $R(100\,\mathrm{K})\approx0.83\,\Omega$ for sample $A$ and $B$, respectively. It should be emphasized that such a difference in resistance can qualitatively be explained by the combination of two causes. One, which has an intrinsic origin, arises from the difference in doping level of the crystals,[47] and another is due to the sample dependence of the geometric factor between the resistivity and the measured resistance. Isothermal $I$-$V$ curves have been recorded using a dc four-probe method with a sensitivity of approximately $10^{-10}$ V and a temperature stability better than 5 mK. Currents up to 100 mA have been used without detecting some heating effects from the temperature controller. The magnetic field was aligned with the ion tracks using the well-known dip feature occurring in dissipation for fields parallel to the columnar defects at filling factors $f=B/B_\phi<1$.

## III. RESULTS

We have examined in some detail how $I$-$V$ curves behave around the superconducting transition ($R\equiv\lim_{1\to0}V/I=0$) in magnetic fields less than $B_\phi$. As an example, Fig. 3 shows a double-logarithmic plot of isothermal $I$-$V$ curves obtained at $B=0.85\,\mathrm{T}$ in the sample $A$ ($B_\phi=1.5\,\mathrm{T}$). One can notice a nonlinear behavior of the curves at lower temperatures, whereas the upper curves exhibit a linear regime. The straight (curved) lines display a least-squares fit of Ohm's

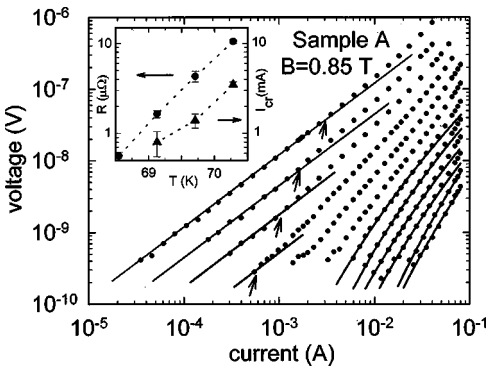


FIG. 3. Double-logaritmic plot of isothermal $I$-$V$ curves for $B$ fixed. From the right to the left $T=63.958$, 64.531, 65.105, 65.679, 66.253, 66.828, 67.403, 67.978, 68.553, 69.129, 69.705, and 70.281 K. The straight lines display a fit of Ohm laws, and the arrows indicate Ohmic–non-Ohmic crossover. The curved lines are a fit according to Eq. (2) (with $\mu=1/3$) to the data obtained for weak currents. Inset: $R$ and $I_{cr}$ vs $T$. The dotted lines are a guide for the eyes.

law [Eq. (2)] to the data obtained for weak currents and higher (lower) temperatures. The inset of the figure shows $R$ as a function of $T$. It may be seen that $R$ vanishes abruptly. The inset also shows $I_{cr}$ separating the Ohmic regime from the non-Ohmic regime as a function of $T$. Here $I_{cr}$ is determined by measuring, within the experimental errors, the threshold current, for which the ratio of $V/I$ to $R$ departs from unity. The result is that $I_{cr}$ vanishes in the same manner as $R$. Such typical behaviors can be explained on the basis of the Bose-glass melting theory.[20]

### A. Universal critical scaling of the resistivity near the Bose-glass transition

In the above approach, one expects that near $T_{BG}$ the resistivity should obey the following ansatz:[20]

$$\frac{\rho}{\rho_0^*}|t|^{-\nu'(z'-\alpha)}=F_\pm\left(\frac{J}{J^*}\right), \tag{1}$$

where the $\pm$ subscript means above and below $T_{BG}$, respectively. In Eq. (1), $t$ denotes the reduced temperature $(T-T_{BG})/T_{BG}$, $z'$ and $\nu'$ are the critical exponents governing the time relaxation and transverse correlation length of fluctuations, respectively, the exponent $\alpha$ accounts for the scaling form $l_\parallel\sim l_\perp^\alpha$ between the longitudinal correlation length and the transverse correlation length, and $\rho_0^*$ is a flux-creep resistivity scale. In the functions $F_\pm(x)$, the current density is scaled by $J^*=J_0^*|t|^{\nu'(1+\alpha)}$ with $J_0^*=k_BT/(\phi_0 l_{0\parallel}l_{0\perp})$. Here $J^*(T)$ defines a current crossover corresponding to a balance between the thermal energy and the work done by the Lorentz force acting on typical vortex-loop fluctuations of area $\sim l_{0\parallel}l_{0\perp}|t|^{-\nu'(1+\alpha)}$. Note that the current effects are always dominant with respect to thermal effects very near $T_{BG}$ because $J^*$ vanishes at $T=T_{BG}$. Both scaling functions $F_\pm(x)$ are unknown analytic functions; their asymptotic behaviors are nevertheless well known.[20] One expects $F_\pm(x)\sim x^{(z'-\alpha)/(1+\alpha)}$ as $x\to\infty$ with the result that $\rho\sim J^{(z'-\alpha)/(1+\alpha)}$ remains finite at $T=T_{BG}$, $F_+(x)\to$const as

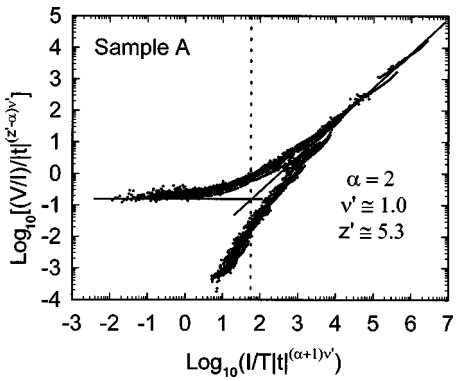


FIG. 4. Scaling forms for the resistivity above and below $T_{BG}$ at different filling factors $f=0.026$, 0.04, 0.066, 0.133, 0.200, 0.266, 0.333, 0.466, 0.566, 0.666, and 0.900. The solid lines represent asymptotic behaviors, and their crossing identifies the quantity $J_0^*$ for $T>T_{BG}$.

$x\to 0$, leading to an Ohmic resistivity, as expected just above $T_{BG}$ in a thermally dominated vortex liquid, and $F_-(x)\sim\exp(1/x^{1/3})$ as $x\to 0$, as required by the variable-range hopping prediction.

Technically, the problem of measuring the critical exponents $z'$ and $\nu'$ by fitting Eq. (1) to the data is difficult because $F_\pm(x)$ are unavailable at present. In preference to any numerical sophisticated treatment, we determine $z'$, $\nu'$, and $T_{BG}$ by the following simple procedure. First, we assume that $J_0^*/T$ and $\rho_0^*$ are sample-dependent constants, independent of $T$ and $B$, along the Bose-glass melting line. Such an hypothesis is based upon the well-known standard universality rules applicable to second-order transitions, which imply that different fields less than $B_\phi$ should correspond to a unique vortex system. We therefore expect that the anisotropic length scales in the system exhibit only one implicit field dependence through $T_{BG}(B)$ in such a way that both $l_\perp$ and $l_\parallel$ are independent of the magnetic field for $(T-T_{BG})/T_{BG}$ fixed. It follows that both $l_{0\parallel}$ and $l_{0\perp}$ (and therefore $J_0^*$) should be independent of $B$. Second, we state that $\rho_0^*$ is comparable in magnitude to the normal resistivity $\rho_n$ and define $J_0^*$ by a simple method: we assume $F_\pm(x)=x^{(z'-2)/3}$ for $x\gg 1$ and $F_+(x)=1$ for $x\ll 1$, where $x\equiv\tilde{I}/\tilde{I}_0^*=J/J^*$ with the relation $\tilde{I}\equiv I/(T|t|^{3\nu'})$ and $\tilde{I}_0^*\equiv AJ_0^*/T$, where $A$ is a sample-dependent constant. Thus we obtain in this way $J_0^*/T$ directly from the asymptotic behaviors of $F_+$. It should also be stated that we set $\alpha=2$ in order that the compressional modulus of the vortex-liquid phase $c_{11}\approx(k_BTB^2/\phi_0^2)l_\perp^2/l_\parallel$ remains finite at $T=T_{BG}$, in accordance with the ideas of Nelson and Vinokur.[20] So the only free parameters are $z'$, $\nu'$, and $T_{BG}$. Using this procedure over a wide range of filling factors $<1$ investigated in both crystals, we succeed in superimposing the data onto a unique experimental curve, as shown in Fig. 4 for sample *A*. Upper $(T>T_{BG})$ and lower $(T<T_{BG})$ branches are associated with $F_+$ and $F_-$, respectively, and the horizontal and oblique solid lines show $F_+(x)=1$ and $F_\pm(x)=x^{(z'-2)/3}$, respectively. Their intersection point gives $\tilde{I}_0^*$ wherefrom we estimate $(l_{0\perp}l_{0\parallel})^{1/2}$; in both samples, we obtain $(l_{0\perp}l_{0\parallel})^{1/2}\approx 15-20$ Å, which are physical values. Moreover, Fig. 4 clearly shows that the postulated form $\rho=\rho_0^*t^{(z'-\alpha)\nu'}$ as $T\to T_{BG}^+$, where $\rho_0^*\sim\rho_n$ is independent of $T$ and $B$, holds for a physical extrapolation of the upper branch. The main finding is that for both samples $z'$ and $\nu'$ are independent of the filling factor, as listed in Table I. Moreover, $z'$ and $\nu'$ appear to be independent, within the experimental errors, of $B_\phi$ and $x$, i.e., the defect density and the yttrium concentration in the material, respectively. We note that the absence of both field and sample dependences in the exponents $z'$ and $\nu'$ is consistent with hypothetical universal critical behavior at the Bose-glass–to–liquid transition.[20] The values $z'=5.28\pm 0.05$ and $\nu'=1.04\pm 0.06$ obtained here agree rather closely with the exponents $z'=6\pm 0.5$ and $\nu'=1.00\pm 0.01$ obtained from numerical simulations[48] and are in good agreement with those obtained in $Tl_2Ba_2CaCu_2O_{8-\delta}$ (Tl-2212) thin films,[37] whereas there exists a large scatter in reported values.[26–32,37] Recently, Mazilu *et al.*[26] reported $z'$

TABLE I. Measured exponents and critical temperature at different filling factors.

| $f=\frac{B}{B_\phi}$ | Sample *A* | | | Sample *B* | | |
|---|---|---|---|---|---|---|
| | $z'\pm 0.05$ | $\nu'\pm 0.06$ | $T_{BG}\pm 0.1$ K | $z'\pm 0.05$ | $\nu'\pm 0.06$ | $t_{BG}\pm 0.1$ K |
| 0.026 | 5.30 | 0.97 | 76.5 | | | |
| 0.040 | 5.27 | 0.97 | 75.2 | | | |
| 0.066 | 5.25 | 0.95 | 73.1 | 4.85 | 0.92 | 81.0 |
| 0.133 | 5.30 | 1.02 | 71.6 | 5.30 | 1.05 | 71.9 |
| 0.200 | 5.25 | 0.95 | 71.2 | | | |
| 0.266 | 5.30 | 1.00 | 70.0 | 5.27 | 1.10 | 70.4 |
| 0.333 | 5.25 | 0.95 | 69.9 | | | |
| 0.400 | | | | 5.30 | 1.10 | 69.3 |
| 0.466 | 5.25 | 1.00 | 68.6 | | | |
| 0.533 | | | | 5.30 | 1.10 | 67.3 |
| 0.566 | 5.30 | 1.05 | 66.9 | | | |
| 0.666 | 5.30 | 1.05 | 65.0 | 5.30 | 1.15 | 65.2 |
| 0.800 | | | | 5.27 | 1.15 | 62.8 |
| 0.900 | 5.30 | 1.12 | 59.3 | | | |

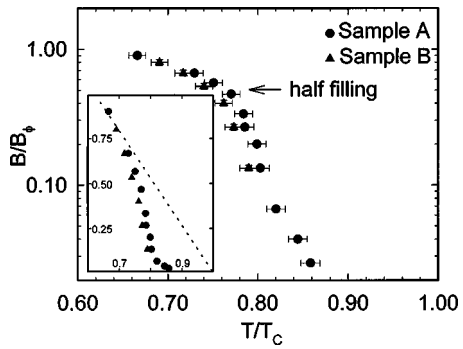


FIG. 5. Log-linear plot of the Bose-glass melting line for both samples scaled to their respective matching field $B_\phi$. A clear crossover is seen close to the half filled regime. Insert shows the figure to linear scale. The dotted line is a guide for the eyes.

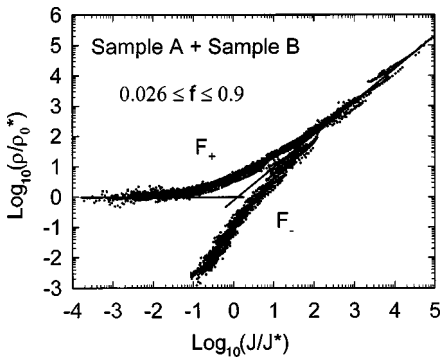


FIG. 6. Universal scaling forms for the resistivity obtained in both samples at filling factors ($f \equiv B/B_\phi$). The exponent values $z' = 5.28 \pm 0.05$ and $\nu' = 1.04 \pm 0.06$ hold for all filling factor ranging from the heavily underfilled regime to the nearly filled regime. $F_+$ and $F_-$ are scaling functions above and below the critical temperature $T_{\mathrm{BG}}$, respectively. The solid lines represent asymptotic behaviors, and their crossing occurs at the normalized point (0,0). Here $\rho_0^*$ is field independent and $J^*$ exhibits an implicit field dependence through $T_{\mathrm{BG}}(B)$. For $T > T_{\mathrm{BG}}$, the physical meaning of the quantities $\rho_0^*$ and $J^*$ is clear: the former accounts for the linear resistivity, and the latter is the current crossover separating the linear regime from the nonlinear regime.

$\approx 7.2$ and $\nu' \approx 1.2$ for YBCO thick films. Budhani *et al.*[29] found $z' = 4.4 \pm 0.3$ and $\nu' = 1.8 \pm 0.2$ for Tl-2212 thin films. Miu *et al.*[30] obtained $\nu'(z'-2) \approx 9$ for BSCCO films, and Seow *et al.*[31] reported a similar value $[\nu'(z'-2) \approx 8.5]$ for BSCCO crystals from out-of-plane transport measurements. However, the exponents $z' \approx 2.2-2.3$, $\nu' \approx 0.9-1$, and $\alpha \approx 1.1-1.2$, implying an incompressible Bose glass, were obtained for YBCO crystals[27,32] as compared to $z' \approx 5.7$, $\nu' \approx 1.8$, and $\alpha = 5/3$ obtained for YBCO thin films.[28] In the present experimental work, the only field-dependent adjustable parameter is $T_{\mathrm{BG}}$ in such a way that $T_{\mathrm{BG}}(B)$ defines the Bose-glass line transition in the $B$-$T$ plane. Figure 5 and its inset show a semilogarithmic plot and a linear plot of $T_{\mathrm{BG}}$ scaled by $T_c$ as a function of the filling factor, respectively. We find that the Bose-glass lines can be scaled to one another as observed elsewhere in BSCCO crystals.[31] Moreover, we observe close to the half filling a well-defined crossover separating an almost linear behavior above $B_\phi/2$ from an upward curvature below, as shown in the inset of Fig. 5. Such a remarkable crossover at a field $B_{\mathrm{cr}} \sim B_\phi/2$ has already been observed in investigations of the irreversibility line in YBCO crystals and BSSCO crystals with columnar defects.[19,33,34] $B_{\mathrm{cr}}$ was related to $B^*$ separating the single-vortex regime from the collective pinning regime, in accordance with the ideas of Nelson and Vinokur.[20] Indeed, as will be seen below, our experimental findings support the relevancy of this scenario. Finally, Fig. 6, whose axes are normalized such that the resistivity is measured in units of $\rho_0^*$ and the current in units of $J^*$, shows that the data obtained from both samples can be superimposed on a unique curve. This result, which holds for filling factors varying from the heavily underfilled regime to the nearly filled regime, is consistent with the scaling theory of the Bose-glass–to–liquid transition.[20]

### B. Variable-range vortex hopping

Below $T_{\mathrm{BG}}$, one expects a nonlinear thermally actived flux-creep resistivity

$$\rho = \rho_0 \exp\left[ -\frac{2E_K}{k_B T} \left( \frac{J_0}{J} \right)^{\mu} \right], \tag{2}$$

where $\rho_0$ is a characteristic flux-creep resistivity, $E_K$ is a kink energy, and $J_0$ is a current scale. The value of the glass exponent $\mu$ is typical of vortex-loop excitations, e.g., $\mu = 1$ for half loops and $\mu = 1/3$ for double superkinks.[20] Over a wide filling range $0.04 \leqslant f \leqslant 0.9$, Fig. 7 shows $d[\ln(V/I)]/dI$ versus $I$ for $T < T_{\mathrm{BG}}$. It should be noted that such log-log plots should indeed be an appropriate way to determine $\mu$ as may be seen by calculating the logarithmic derivative of Eq. (2) with respect to $J$, namely, $d[\ln \rho]/dJ \propto (J_0/J)^{\mu+1}$. In Fig. 7, the solid lines are a least-squares fit of a power law to the data. We obtain in this way $\mu = 0.33 \pm 0.06$. As a comparison, the dashed lines represent an attempt to fit $d[\ln \rho]/dJ \propto (J_0/J)^{\mu+1}$, where $\mu = 1$, to the data. We note that the central value $\mu = 1/3$ is valid throughout the filling range investigated. This result also applies to sample *B*. Such a value for $\mu$ is the very signature of a variable-range vortex hopping transport as predicted in a Bose glass with short-range interaction effects, in the limit of weak current densities.[20] Täuber

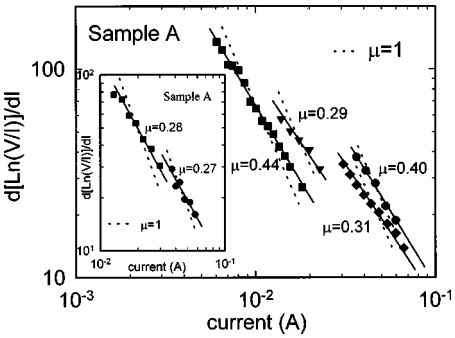


FIG. 7. Log-log plot of $d\ln(V/I)/dI$ vs $I$ for $B$ and $T$ fixed in the Bose-glass phase (■ $f = 0.9$, $T = 58.809$ K; ◆ $f = 0.9$, $T = 57.098$ K; ▼ $f = 0.04$, $T = 74.902$ K; ● $f = 0.04$, $T = 72.589$ K). The straight lines are regression lines wherefrom we obtain the glassy exponent $\mu = 0.33 \pm 0.06$. Inset: ■ $f = 0.566$, $T = 66.253$ K; ● $f = 0.2$, $T = 68.553$ K.

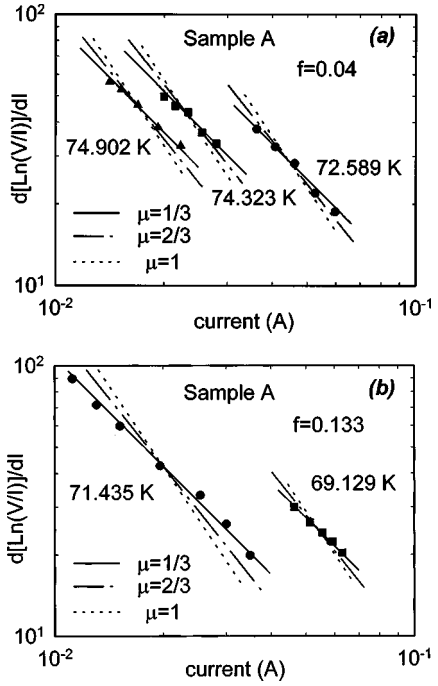


FIG. 8. Log-log plot of $d\ \ln(V/I)/dI$ vs $I$ for $B$ and $T$ fixed in the strongly underfilled Bose-glass regime with long-range interactions $\lambda_{ab}/d \approx 10$. (a) $f=0.04$ and (b) $f=0.133$. The straight lines are regression lines for some typical values of the glassy exponent $\mu$ (see the text). The finding is that no Coulomb gap appears in the distribution of pinning energies.

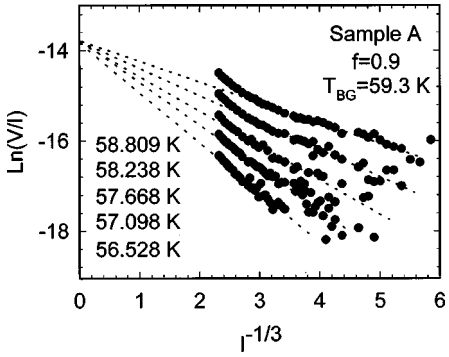


FIG. 9. $\ln(V/I)$ vs $I^{-1/3}$ for $B$ and $T$ fixed within the Bose-glass phase. Dashed lines are a least-squares fit of Eq. (2) (with $\mu=1/3$) to the data. Note that the dashed lines intersect at a single point lying on the ordinate axis wherefrom we obtain $R_0$ (see Table II).

and Nelson[39] and Wengel and Täuber[40] have shown using numerical simulations that the analogue of the Coulomb gap[23] should appear in the distribution of pinning energies, arising from long-range repulsive interaction effects, with the result that $\mu$ varies over the interval 1/3–1. For example, they have found that for ratios of the in-plane penetration depth to the mean distance between the pins, $\lambda_{ab}/d$, varying over the interval 0.5–5, $\mu$ monotonously increases from $\mu \approx 0.52$ to $\mu \approx 0.74$ for $f=1$ and from $\mu \approx 0.43$ to $\mu \approx 0.71$ for $f=0.6$,[40] whereas $\mu$ reaches an upper value of $\sim 2/3$ as $\lambda_{ab}/d \geqslant 5$ for low filling factors ($f<0.1$).[39] We do not observe this feature, as shown in Figs. 8(a) and 8(b) where the noninteracting result $\mu=1/3$ still holds for low filling fractions $0.04 \leqslant f \leqslant 0.133$ and long-range interactions $\lambda_{ab}/d \geqslant 10$. Two possible explanations can at least be given. One is that the dispersion of pinning energies essentially arises from some disorder effect. Note that the weakening of the vortex-vortex interaction in the presence of columnar defects[49] gives an added effect to this situation. Another reason is that the measurements have been done at high temperatures ($T/T_c \approx 0.8$) where the wandering of vortex lines, neglected in Refs. 39 and 40, is here expected to be increased significantly due to thermal fluctuations. Finally, taking $\mu=1/3$ and substituting for $\mu$ into Eq. (2), we fit Eq. (2) to the data. In this way, we introduce here only two independent fitting parameters. One corresponds to the quantity $E_K J_0^{1/3}$, and the other denoted as $R_0$ is proportional to $\rho_0$; namely, $R_0 = A' \rho_0 / w$, where $w$ is the thickness of the crystal and $A'$ is a dimensionless geometric factor which depends on the contact configuration. As an example, the dotted straight lines shown in Fig. 9 are regression lines obtained at $f=0.9$ for sample $A$. According to theoretical predictions, we note that the variable-range hopping model fails to account for the data at higher currents. In Fig. 9, the slope of every dashed line is related to the quantity $(2E_K/k_BT)J_0^{1/3}$, while their intersection with the axis of the ordinates gives $R_0$. It can be inferred that $R_0$ is constant for $B$ fixed. The resulting $R_0$ values are listed for different filling factors in Table II. It may be seen that $R_0$ is only sample dependent (within the error bars). We obtain $R_0 \approx 0.9 \pm 0.2\ \mu\Omega$ for sample $A$ and $R_0 \approx 1.7 \pm 0.3\ \mu\Omega$ for sample $B$. Note that the product of $R_0$ and $w$ is roughly equal to a constant ($R_0 w \sim 10^{-11}\ \Omega$ m). This suggests an independence of $\rho_0$ with respect to the sample. Such a very low estimate for $\rho_0$, which is five orders of magnitude lower than the normal resistivity, accounts for the smallnest of the creep resistivity scale as expected in a Bose glass. Finally, for sample $A$ the values of the fitting parameter related to the quantity $(2E_K/k_BT)J_0^{1/3}$, as described above, are displayed for different temperatures and filling factors in Fig. 10.

TABLE II. Measured prefactor of Eq. (2) at different filling factors.

| $f=\frac{B}{B_\phi}$ | SAMPLE $A$ $R_0\ (\mu\Omega)$ | SAMPLE $B$ $R_0\ (\mu\Omega)$ |
|---|---|---|
| 0.026 | $0.9 \pm 0.2$ | |
| 0.040 | $0.8 \pm 0.2$ | |
| 0.066 | $0.7 \pm 0.2$ | $2.2 \pm 0.3$ |
| 0.133 | $0.8 \pm 0.2$ | $1.5 \pm 0.3$ |
| 0.200 | $0.9 \pm 0.2$ | |
| 0.266 | $1.0 \pm 0.2$ | $1.2 \pm 0.3$ |
| 0.333 | $1.2 \pm 0.2$ | |
| 0.400 | $0.8 \pm 0.2$ | $2.2 \pm 0.3$ |
| 0.466 | $1.0 \pm 0.2$ | |
| 0.533 | | $1.5 \pm 0.3$ |
| 0.566 | $1.3 \pm 0.2$ | |
| 0.666 | $0.8 \pm 0.2$ | $1.6 \pm 0.3$ |
| 0.800 | | $1.8 \pm 0.3$ |
| 0.900 | $1.0 \pm 0.2$ | |

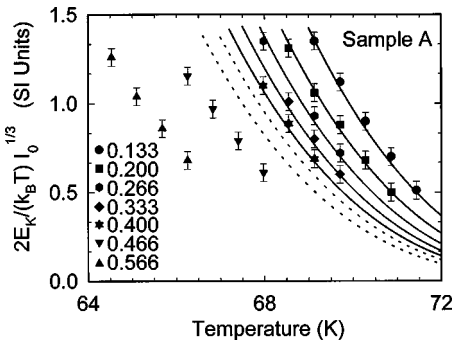


FIG. 10. $2E_K/(k_BT)I_0^{1/3}$ vs $T(T<T_{BG})$ for different filling factors. The lines display a fit of the model described in the text. Theoretical curves and experimental data quantitatively agree in the underfilled regime ($f<1/2$). The dotted lines are associated with $f=0.466$ and $f=0.566$. This breakdown accounts for the crossover from a strongly pinned Bose glass to a weakly pinned Bose glass. It occurs close to the half-filled regime and is probably related to the well-defined crossover in the Bose-glass melting line (see Fig. 5).

## IV. DISCUSSION

To test the accuracy of the above view, we estimate from the model[20] the typical kink energy and the characteristic current in Eq. (2).

The kink energy $E_K$ is given by

$$E_K = d\sqrt{\tilde{\varepsilon}_1 U}, \tag{3}$$

with $d\approx\sqrt{\phi_0/B_\phi}$ being the mean distance between defects, $\tilde{\varepsilon}_1\approx\varepsilon\varepsilon_0\ln(a_0/\xi_{ab})$ being the tilt modulus where $\varepsilon$ is the anisotropic parameter, $\varepsilon_0=\phi_0^2/(4\pi\mu_0\lambda_{ab}^2)$ is the line tension, $a_0\approx\sqrt{\phi_0/B}$ is the vortex-lattice parameter, $U=U_0 f(T/T^*)$ being the binding free energy per unit length where $U_0$ is the mean pinning energy, $T^*=\max[c_0,\sqrt{2}\xi_{ab}]\sqrt{\tilde{\varepsilon}_1 U_0}$ is the energy scale for the pinning, and $f(x)=(x^2/2)\exp(-2x^2)$ accounts for thermal effects.

In Eq. (2), $J_0=1/[\phi_0 g(\tilde{\mu})d^3]$, where $g(\tilde{\mu})$ denotes the density of pinning energies at the chemical potential separating the occupied defects from the empty defects. Note that $g(\varepsilon)$ is normalized such that $\int_{-\infty}^{+\infty}g(\varepsilon)d\varepsilon=1/d^2$. Although a form of $g(\varepsilon)$ is not yet available, an estimation of $g(\tilde{\mu})$ can be done in terms of $\gamma$, the bandwidth of pinning energies. An intrinsic dispersion in the pinning energies originates from the combined effects between vortex repulsion and disorder. The field-independent value of the glass exponent $\mu\approx1/3$ suggests that $\gamma$ is mainly due to the disorder effect. Thus we can consider $g(\varepsilon)$ as a smooth function near $\tilde{\mu}$.[39,40] Then we have approximately $g(\tilde{\mu})\approx1/(d^2\gamma)$, wherefrom we obtain

$$J_0\approx\gamma/[\phi_0 d]. \tag{4}$$

In Eq. (4), $\gamma$ should be given by the combination of energy dispersions arising from some structural and on-site disorders:[1]

$$\gamma\approx t_d+\gamma_i. \tag{5}$$

An estimate for the energy dispersion due to the structural disorder, i.e., the randomness in the distance between the irradiation tracks, has been made in terms of the hopping matrix element connecting sites separated by the typical distance $d$,[20]

$$t_d\approx\sqrt{\sqrt{2}/\pi}\frac{U}{\sqrt{E_K/k_BT}}\exp\left(-\frac{\sqrt{2}E_K}{k_BT}\right). \tag{6}$$

On the other hand, assuming the variation in the defect diameters as the first cause for random on-site energies (see Fig. 1), we approximate, in Eq. (5), $\gamma_i$ to the width of the distribution of pinning energies:

$$\tilde{P}(U_k)=P(c_k)\frac{dc_k}{dU_k}. \tag{7}$$

In Eq. (7), the pinning energy per unit length, $U_k$, and the defect radius $c_k$ are related to one another through the formula[20]

$$U_k=\frac{\varepsilon_0}{2}\ln[1+(c_k/\sqrt{2}\xi_{ab})^2], \tag{8}$$

and $P(c_k)$ define a distribution of defects, such that $N(c_k)=\int_0^{c_k}P(c_k')dc_k'$ is the number of columnar defects per unit area with radius less than $c_k$. Note that $P(c_k)$ is normalized such that $N(+\infty)=1/d^2$.

Applying Eqs. (3)–(8) and assuming a normal law for $P(c_k)$, we have attempted to fit the quantity $(E_K/T)J_0^{1/3}$ to the data. We have worked out a least-squares fit with five fitting parameters: the average defect radius $c_0=\langle c_K\rangle$, the standard deviation of $c_K$, the anisotropy parameter $\varepsilon$, and both the in-plane penetration depth and the in-plane coherence length at $T=0$. Indeed, Fig. 10 shows that the experimental data obtained at filling factors $<1/2$ quantitatively agree with the theoretical curves. This result also applies to sample *B*. Here note that we have used the temperature dependence as predicted in the two-fluid model for the in-plane penetration depth, i.e., $\lambda_{ab}(T)=\lambda_{ab}(0)[1-(T/T_c)^4]^{-1/2}$. For both samples, the optimum fitting parameter values are listed in Table III. Two significant points can be noted. Mainly, we obtain an average defect diameter $2c_0=90\pm4$ Å with a standard deviation $\sigma=15\pm3$ Å that is strongly consistent with the probability law for the defect diameter $c_K$ obtained from high-resolution electron microscopy, as shown in Fig. 1. Second, the only sample-dependent quantity is $\lambda_{ab}(0)$. Neglecting the effective renormalization of the penetration depth due to defects,[49] the sample dependence of

TABLE III. Fitting parameters.

| Sample | $c_0$ (Å) | $\sigma/c_0$ (%) | $1/\varepsilon$ | $\lambda_{ab}(0)$ (Å) | $\xi_{ab}(0)$ (Å) |
|---|---|---|---|---|---|
| *A* | 45±2 | 17.5±2.5 | 50±2 | 1790±20 | 17±2 |
| *B* | 45±2 | 16±2.5 | 52±2 | 1910±20 | 15±2 |

$\lambda_{ab}(0)$ can qualitatively be explained in terms of different doping levels.[47] Then the corresponding $\lambda_{ab}(0)$ values clearly show that the in-plane penetration depth decreases as the hole doping is increased, as expected in the underdoped regime.[50]

To conclude, we discuss in more detail the origin of the variable-range vortex hopping transport. Using the fitting parameter values listed in Table III and applying Eqs. (3) and (6)–(8), we draw a comparison between $t_d$ and $\gamma_i$ in Eq. (5). In this way, we find that $\gamma_i$ is still much greater than $t_d$ for all temperatures and filling factors. As an example, at $T=70\,\mathrm{K}$ and for $0.1\leqslant f\leqslant 0.4$, the ratio of $\gamma_i$ to $t_d$ varies from 100 to 200. Thus we conclude that the dispersion in the pinning energies, which results in the variable-range hopping process, essentially arises from on-site (i.e., diagonal) disorder.

However, this conclusion is only valid for the underfilled Bose-glass regime where all the vortices are strongly bounded to the columnar defects. Obviously, such an argument breaks down in the case of the weak Bose-glass regime where some vortices are localized by energetically favorable interstitial sites due to the vortex-vortex interaction. Therefore, it must be kept in mind that the above model should no longer be valid for $B\geqslant B^*$. Indeed, it may be seen in Fig. 10 that the theoretical curves and the experimental data quantitatively agree as long as the inequality $f<1/2$ holds. Such a result is also verified for sample *B*. This strongly suggests that for the interaction range ($\lambda_{ab}/d\approx 10$) probed in our experiment, $B^*/B_\phi\sim 1/2$. Such an estimate of $f^*$ remarkably agrees with that obtained from numerical simulations, as may be seen by using the Fig. 1 shown in Ref. 40(a). In addition, it should be emphasized that the Bose-glass melting line also exhibits a crossover at $B_{cr}\sim B_\phi/2$, as shown in Fig. 5. This is not probably coincidental, and thus $B_{cr}$ is consistent with $B^*$, in accordance with other experimental works.[33,34]

## V. SUMMARY

In this work, two important features of the vortex transport in $Bi_2Sr_2Ca_{1-x}Y_xCu_2O_{8+\delta}$ single crystals with columnar defects along the *c* axis have experimentally been investigated from current-voltage measurements. First, the critical behavior of the superconducting phase transition has been studied for magnetic fields ($B<B_\phi$) aligned with the defects. The critical exponents $\nu'(\equiv\nu_\perp)$, $\alpha(\equiv\nu_\parallel/\nu_\perp)$, and $z'$ and the critical temperature $T_{BG}$ have been determined using the scaling hypothesis of the glass transition. Field and matching field-independent values $z'=5.28\pm0.05$, $\nu'=1.04\pm0.06$, and $\alpha=2$ have been found to be in good agreement with those predicted to the Bose-glass–to–liquid transition from numerical simulations. This result is compatible with the well-established universality rules for the critical exponents at standard continuous transitions, since both different fields and matching fields correspond to a unique vortex system. Another finding is that the anisotropic length scale is independent of *B* for $T-T_{BG}/T_{BG}$ fixed, as expected in the presence of a true critical region along $T_{BG}(B)$. A third result is that the resistivity, obtained for both different fields ($B<B_\phi$) and matching fields as a function of temperature, collapses into two single curves when plotted using the rescaled axes according to Eq. (1). All these experimental findings are consistent with a critical behavior of the resistivity that one would expect if the Bose-glass–to–liquid transition was governed by the usual second-order transition universality rules. The experimental evidence of these rules clearly requires further investigation.

Second, the behavior of the conductivity at $T<T_{BG}$ has been examined in some detail for different filling factors $(B/B_\phi)<1$. A variable-range vortex hopping mechanism typical of a Bose glass has clearly been observed, in accordance with the theoretical prediction of Nelson and Vinokur. The glass exponent value $\mu\approx 1/3$ has been found over a wide filling factor range from 0.04 to 0.9 for long-range interactions $\lambda_{ab}/d\sim 10$. This suggests that no Coulomb-gap-like feature occurs in the distribution of pinning energies. Such a conclusion is compatible with a compressible Bose glass as inferred from the above finding that $\alpha=2$, since a divergence of $c_{11}$ can be connected to a gap in the density of vortex states.[40] Finally, the origin of the variable-range hopping mechanism has quantitatively been discussed in terms of the bandwidth of the pinning energies arising from some disorder effect. So we have demonstrated the experimental evidence that for filling factors $<1/2$ the on-site disorder plays a major role. Our finding supports the view of an underfilled Bose-glass regime ($B/B_\phi<1/2$) in which the vortices are strongly localized on the columnar defects, followed by a crossover to a regime of weak localization due to interaction effects. It is probably no coincidence that the Bose-glass melting line also exhibits a crossover near the half filling factor, as shown in Fig. 5. In accordance with numerical simulations, this crossover from a strongly to a weakly pinned Bose-glass regime is found to be consistent with the field $B^*$ introduced in Ref. 20.

*Author to whom correspondence should be addressed. Electronic address: soret@delphi.phys.univ-tours.fr

†Unité Propre de Recherche de l'Enseignement Supérieur associée au CNRS et Laboratoire de Recherche Correspondant du CEA.

‡Unité Mixte de Recherche associée au CNRS, à l'ISMRA et à l'Université de Caen.

[1] G. Blatter, M. V. Feigel'man, V. B. Geshkenbein, A. I. Larkin, and V. M. Vinokur, Rev. Mod. Phys. **66**, 1125 (1994).

[2] A. Larkin, Zh. Eksp. Teor. Fiz. **58**, 1466 (1970) [Sov. Phys. JETP **31**, 784 (1970)].

[3] A. E. Koshelev and V. M. Vinokur, Phys. Rev. Lett. **73**, 3580 (1994).

[4] T. Giamarchi and P. Le Doussal, Phys. Rev. Lett. **76**, 3408 (1996); P. Le Doussal and T. Giamarchi, Phys. Rev. B **57**, 11 356 (1998).

[5] S. Scheidl and V. M. Vinokur, Phys. Rev. B **56**, R8522 (1997); **57**, 13 800 (1998); Phys. Rev. E **57**, 2574 (1998).

[6] M. V. Feigel'man, V. B. Geshkenbein, A. I. Larkin, and V. M. Vinokur, Phys. Rev. Lett. **63**, 2303 (1989).

[7] M. P. A. Fisher, Phys. Rev. Lett. **62**, 1415 (1989); R. H. Koch, V. Foglietti, W. J. Gallager, G. Koren, A. Gupta, and M. P. A. Fisher, *ibid.* **63**, 1511 (1989); D. S. Fisher, M. P. A. Fisher, and D. A. Huse, Phys. Rev. B **43**, 130 (1991).

[8] T. Giamarchi and P. Le Doussal, Phys. Rev. Lett. **72**, 1530

(1994); Phys. Rev. B **52**, 1242 (1995); **55**, 6577 (1997).
[9] T. D. Ertaş and D. R. Nelson, Physica C **272**, 79 (1996).
[10] J. Kierfeld, T. Nattermann, and T. Hwa, Phys. Rev. B **55**, 626 (1997).
[11] D. S. Fisher, Phys. Rev. Lett. **78**, 1964 (1997).
[12] Atomic impurities, such as oxygen vacancies, should be an important source of uncorrelated disorder in high-temperature superconducting cuprates due to their short coherence lengths.
[13] S. Ryu, A. Kapitulnik, and S. Doniach, Phys. Rev. Lett. **77**, 2300 (1996).
[14] B. Khaykovich, E. Zeldov, D. Mayer, T. W. Li, P. H. Kes, and M. Konczykowski, Phys. Rev. Lett. **76**, 2555 (1996); B. Khaykovich, M. Konczykowski, E. Zeldov, R. A. Doyle, D. Mayer, P. H. Kes, and T. W. Li, Phys. Rev. B **56**, R517 (1997).
[15] K. Deligiannis, P. A. J. de Groot, M. Oussena, S. Pinfold, R. Langan, R. Gagnon, and L. Taillefer, Phys. Rev. Lett. **79**, 2121 (1997).
[16] R. Cubitt, E. M. Forgan, G. Yang, S. L. Lee, D. McK. Paul, H. A. Mook, M. Yethiraj, P. H. Kes, T. W. Li, A. A. Menovsky, Z. Tarnawski, and K. Mortensen, Nature (London) **365**, 407 (1993).
[17] V. Hardy, D. Grould, M. Hervieu, J. Provost, B. Raveau, and S. Bouffard, Nucl. Instrum. Methods Phys. Res. B **54**, 472 (1991).
[18] L. Civale, A. D. Marwick, T. K. Worthington, M. A. Kirk, J. R. Thompson, L. Krusin-Elbaum, Y. Sun, J. R. Clem, and F. Holtzberg, Phys. Rev. Lett. **67**, 648 (1991); M. Konczykowski, F. Rullier-Albenque, E. R. Yacoby, A. Shaulov, Y. Yeshurun, and P. Lejay, Phys. Rev. B **44**, 7167 (1991).
[19] V. Hardy, J. Provost, D. Groult, M. Hervieu, B. Raveau, S. Durčok, E. Pollert, J. C. Frison, J. P. Chaminade, and M. Pouchard, Physica C **191**, 85 (1992).
[20] D. R. Nelson and V. M. Vinokur, Phys. Rev. Lett. **68**, 2398 (1992); Phys. Rev. B **48**, 13 060 (1993).
[21] T. Hwa, P. Le Doussal, D. R. Nelson, and V. M. Vinokur, Phys. Rev. Lett. **71**, 3545 (1993).
[22] M. P. A. Fisher, P. B. Weichman, G. Grinstein, and D. S. Fisher, Phys. Rev. B **40**, 546 (1989).
[23] B. I. Shklovskii and A. L. Efros, *Electronic Properties of Doped Semiconductors* (Springer, Berlin, 1984), and references therein.
[24] L. Radzihovsky, Phys. Rev. Lett. **74**, 4919 (1995); **74**, 4923 (1995).
[25] K. M. Beauchamp, T. F. Rosenbaum, U. Welp, G. W. Crabtree, and V. M. Vinokur, Phys. Rev. Lett. **75**, 3942 (1995); E. R. Nowak, S. Anders, H. M. Jaeger, J. A. Fendrich, W. K. Kwok, R. Mogilevsky, and D. G. Hinks, Phys. Rev. B **54**, R12 725 (1996).
[26] A. Mazilu, H. Safar, M. P. Maley, J. Y. Coulter, L. N. Bulaevskii, and S. Foltyn, Phys. Rev. B **58**, R8909 (1998).
[27] W. Jiang, N. C. Yeh, D. S. Reed, U. Kriplani, D. A. Beam, M. Konczykowski, T. A. Tombrello, and F. Holtzberg, Phys. Rev. Lett. **72**, 550 (1994).
[28] G. Nakielski, A. Rickertsen, T. Steinborn, J. Wiesner, G. Wirth, A. G. M. Jansen, and Kötzler, Phys. Rev. Lett. **76**, 2567 (1996).
[29] R. C. Budhani, W. L. Holstein, and M. Suenaga, Phys. Rev. Lett. **72**, 566 (1994).
[30] L. Miu, P. Wagner, A. Hadish, F. Hillmer, H. Adrian, J. Wiesner, and G. Wirth, Phys. Rev. B **51**, 3953 (1995).
[31] W. S. Seow, R. A. Doyle, A. M. Campbell, G. Balakrishnan, D. McK. Paul, K. Kadowaki, and G. Wirth, Phys. Rev. B **53**, 14 611 (1996).
[32] D. S. Reed, N. C. Yeh, M. Konczykowski, A. V. Samoilov, and F. Holtzberg, Phys. Rev. B **51**, 16 448 (1995).
[33] L. Krusin-Elbaum, L. Civale, G. Blatter, A. D. Marwick, F. Holtzberg, and C. Feild, Phys. Rev. Lett. **72**, 1914 (1994); L. Krusin-Elbaum, L. Civale, J. R. Thompson, and C. Feild, Phys. Rev. B **53**, 11 744 (1996).
[34] D. Zech, S. L. Lee, H. Keller, G. Blatter, B. Janossy, P. H. Kes, T. W. Li, and A. A. Menovsky, Phys. Rev. B **52**, 6913 (1995); D. Zech, S. L. Lee, H. Keller, G. Blatter, P. H. Kes, and T. W. Li, *ibid.* **54**, 6129 (1996).
[35] C. J. van der Beek, M. Konczykowski, V. M. Vinokur, T. W. Li, P. H. Kes, and G. W. Crabtree, Phys. Rev. Lett. **74**, 1214 (1995); M. Konczykowski, N. Chikumoto, V. M. Vinokur, and M. V. Feigelman, Phys. Rev. B **51**, 3957 (1995).
[36] J. R. Thompson, L. Krusin-Elbaum, L. Civale, G. Blatter, and C. Feild, Phys. Rev. Lett. **78**, 3181 (1997).
[37] V. Ta Phuoc, A. Ruyter, L. Ammor, A. Wahl, J. C. Soret, and Ch. Simon, Phys. Rev. B **56**, 122 (1997).
[38] V. V. Moshchalkov, V. V. Metlushko, G. Güntherodt, I. N. Goncharov, A. Yu. Didyk, and Y. Bruynseraede, Phys. Rev. B **50**, 639 (1994); C. J. van der Beek, M. Konczykowski, V. M. Vinokur, G. W. Crabtree, T. W. Li, and P. H. Kes, *ibid.* **51**, 15 492 (1995).
[39] U. C. Täuber and D. R. Nelson, Phys. Rev. B **52**, 16 106 (1995).
[40] (a) C. Wengel and U. C. Täuber, Phys. Rev. Lett. **78**, 4845 (1997); (b) Phys. Rev. B **58**, 6565 (1998).
[41] M. V. Indenbom, C. J. van der Beek, M. Konczykowski, and F. Holtzberg, Phys. Rev. Lett. **84**, 1792 (2000).
[42] A. Ruyter, Ch. Simon, V. Hardy, M. Hervieu, and A. Maignan, Physica C **225**, 235 (1994).
[43] G. Villard, D. Pelloquin, A. Maignan, and A. Wahl, Physica C **278**, 11 (1997).
[44] S. Hébert, V. Hardy, M. Hervieu, G. Villard, Ch. Simon, and J. Provost, Nucl. Instrum. Methods Phys. Res. B **146**, 545 (1998).
[45] J. R. Thompson, David Paul, Z. L. Wang, D. M. Kroeger, and D. K. Christen, Appl. Phys. Lett. **67**, 1007 (1995).
[46] D. T. Fuchs, E. Zeldov, M. Rappaport, T. Tamegai, S. Ooi, and H. Shtrikman, Nature (London) **391**, 373 (1998); D. T. Fuchs, E. Zeldov, T. Tamegai, S. Ooi, M. Rappaport, and H. Shtrikman, Phys. Rev. Lett. **80**, 4971 (1998); R. A. Doyle, S. F. W. R. Rycroft, T. B. Doyle, E. Zeldov, T. Tamegai, and S. Ooi, Phys. Rev. B **58**, 135 (1998); D. T. Fuchs, R. A. Doyle, E. Zeldov, S. F. W. R. Rycroft, T. Tamegai, S. Ooi, M. L. Rappaport, and Y. Myasoedov, Phys. Rev. Lett. **81**, 3944 (1998); A. Mazilu, H. Safar, D. López, W. K. Kwok, G. W. Crabtree, P. Guptasarma, and D. G. Hinks, Phys. Rev. B **58**, R8913 (1998); S. F. W. R. Rycroft, R. A. Doyle, D. T. Fuchs, E. Zeldov, R. J. Drost, P. H. Kes, T. Tamegai, S. Ooi, and D. T. Foord, Phys. Rev. B **60**, R757 (1999).
[47] The substitution of $Y^{3+}$ for $Ca^{2+}$ in $Bi_2Sr_2Ca_{1-x}Y_xCu_2O_{8+\delta}$ varies the doping level of the $CuO_2$ planes from the overdoped to the underdoped regime with an optimum level for $T_c$ at $x \approx 0.28$. See Ref. 50.
[48] M. Wallin and S. M. Girvin, Phys. Rev. B **47**, 14 642 (1993).
[49] A. Buzdin and D. Feinberg, Physica C **256**, 303 (1996).
[50] G. Villard, D. Pelloquin, and A. Maignan, Phys. Rev. B **58**, 15 231 (1998).